THE EFFECT OF COOLING RATE ON THE CRYSTALLIZATION PROCESS OF LIQUID RHODIUM: MOLECULAR DYNAMICS SIMULATIONS

Murat Celtek[1], Unal Domekeli[2], Sedat Sengul[2]
[1]*Faculty of Education, Trakya University, 22030, Edirne - TURKEY*
[2] *Dept. of Physics, Trakya University, 22030, Edirne – TURKEY*

Abstract

In the present study, the microstructural evolution of rhodium during the heating and cooling processes was investigated by molecular dynamic simulation method using the embedded atom potentials. Five different cooling rates were used to investigate the effect of the cooling rate on the crystallization process of the system. All molecular dynamics simulation results were discussed in detail using the pair distribution function, energy temperature curves and pair analysis methods. The results have shown that the cooling rate chosen has a great effect on the development of the atomic structure of the system during the crystallization process and the liquid-solid phase transition temperature of the system.

Keywords: molecular dynamic simulaitons, liquid-solid phase, coolig rate, crystallization.

INTRODUCTION

Many materials such as amorphous and polycrystalline solids are generally prepared by applying solidification process on liquid material. In this case, the speed at which the sample will be cooled is of great importance [1,2]. Understanding what kind of changes occur in the microstructure of metallic melts during solidification is fundamental requirement in both condensed matter and material science [3, 4]. The crystallization of a liquid to form a solid in molecular dynamics (MD) simulations was first observed by Alder et al. [5] for solid sphere liquid and by Mandell et al. [6] for Lennard-Jones liquid, and then many MD simulation studies were carried out on the crystallization process of other liquids. Rhodium (Rh) element is generally used to harden Platinum and Palladium. The alloys it contains are used in laboratories, aircraft technology, and high temperature furnaces. In addition, it is also used in the production of light reflective hard surfaces, optical instruments and tools, decoration, industry and industrial production to increase electrical conductivity. These important properties have increased interest in pure Rh and its alloys both experimentally and theoretically. Although studies have been carried out on the structural development and crystallization process of pure Rh, there are still many points that are not understood about this element. In our present study, local atomic environment in Rh during the heating and cooling processes were examined by MD simulations using the embedded atom method (EAM). Five different cooling rates (10, 5, 1, 0.5 and 0.05 K/ps) were used to investigate the effects of the cooling rate on the crystallization process during the cooling. The pair distribution function (PDF) (or *g(r)*) and the pair analysis (PA) method were used to discuss the changes in the atomic structure of the system in both processes. Results obtained from MD simulations were discussed in detail in later chapters.

EXPOSITION

The EAM potential has been used to describe atomic interactions in the system throughout the MD simulation. The form of EAM representing the total energy of an atomic system is defined as follows [7].

$$E_{tot} = \frac{1}{2}\sum_{ij} V_{ij}\left(r_{ij}\right) + \sum_{i} F_i\left(\bar{\rho}_i\right). \qquad (1)$$

Here $V_{ij}(r_{ij})$ is the pair interaction energy between i and j atoms that are at a distance of r_{ij} from each other. F_i is the embedding energy of atom i, and is defined as a function of the host electron density $\bar{\rho}_i$.

$$\bar{\rho}_i = \sum_{j \neq i} \rho_j\left(r_{ij}\right) \qquad (2)$$

In our study, the EAM data set parameterized by Sheng et al. was used [8]. All MD simulations were employed by DLPOLY open source package program [9]. The initial conditions of Rh were arranged in the ideal face-centered (fcc) structure and a total of 6912 (12x12x12x4) atoms were placed in the cubic cell, and periodic boundary conditions were applied through all three directions of the simulation box. MD simulations were carried out in the NPT ensemble during the heating and cooling processes, and Berendsen thermostat and barostat were used in these processes to keep temperature and pressure under control. In order to determine the new configurations of the atoms in the system, Newton's equations of motion were solved, and time step of 1 fs and Leapfrog Verlet algorithm were used for this. Initially, the system was equilibrated at the room temperature with a 1,000,000 MD step to relieve the stress on the system, and then it was cooled to 0 K in the same MD step. The system was then heated from 0 K to 3200 K with ΔT = 100 K increments. The system, which was ensured to be liquid at 3200 K, was cooled to 300 K with five different cooling rates (10, 5, 1, 0.5 and 0.05 K/ps) and ΔT = 100 K steps. In order to determine both melting and crystallization temperatures (T_c) more sensitively, the temperature decrement was chosen as ΔT = 20 K in the relevant regions.

The temperature-dependent evolution of the total energy per atom obtained during the heating and cooling processes is given in Fig. 1 comparatively. The inset in Fig. 1 depicts only the energy temperature (E-T) curves obtained during the cooling process between 300-1400 K. During the heating, the E-T curve increased almost linearly between 300 K and 2120 K depending on the temperature, while a sudden jump in the E-T curve has been observed between 2120 K and 2140 K. This sudden and sharp change in the E-T curve is a clear indication that the solid Rh has changed its phase and transitioned to a liquid structure. The temperature where this sudden change begins is called the melting temperature (T_m=2120±10 K), while the point where the sudden increase ends is called the liquid temperature (T_l=2140±10 K). There is a very small difference of -5.19% between the T_m = 2120 K obtained from the MD simulation and the experimental T_m = 2236 K [10]. This is an indication that the selected EAM potential can well estimate the liquid properties as well as the solid properties of the system. The E-T curves obtained from the five cooling rates almost overlap with the heating E-T curve in the supercooled and liquid region, reflecting that the atoms can move fast enough at high temperatures for all systems. With the decreasing temperature, changes occur in the slopes of the E-T curves depending on the cooling rate. The first sharp break observed in the E-T curves during the cooling process occurred between 1160-1140 K and 1160-1120 K for the slowest cooling rates of 0.05 and 0.5 K/ps, respectively. This break in E-T curves is very abrupt and sharp, as in the E-T curve obtained from heating. This behavior also indicates that the system transfers from liquid to crystalline structure for these cooling rates. Although similar behavior has been observed for other cooling rates, depending on the cooling rate, changes in the E-T curves become softer compared to slow cooling rates, and these changes become imperceptible at the fastest cooling rates. These slow transitions indicate that the system passes from liquid to a crystal-like structure.

In the present study, the T_c temperatures of the system have been calculated as 760±10, 860±10, 1040±10, 1120±10 and 1140±10 K from the E-T curves for 10, 5, 1, 0.5 and 0.05 K/ps cooling rates, respectively.

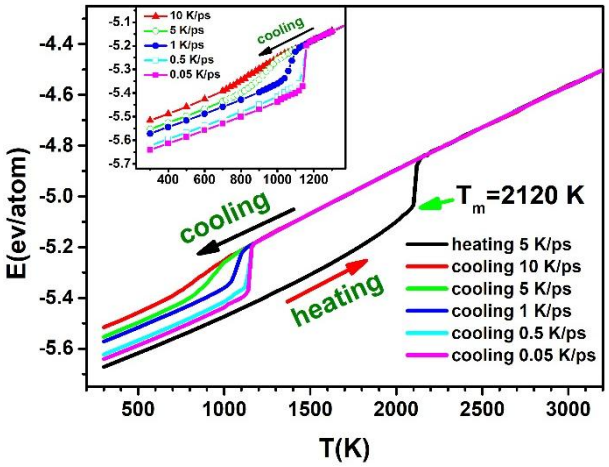

Fig. 1. *Evolution of energy curves as a function of temperature during the heating and cooling process.*

T_c temperatures determined as a function of the logarithm of the cooling rate for Rh are given in Fig. 2. No linear relationship has been observed between the cooling rate and T_c. Instead, it has been observed that as the cooling rate of the system decreases, the crystallization temperature point increases parabolically towards higher temperatures. This result is related to the MD simulation step that is introduced to the system in the cooling process, that is, the increase in the time allowing the system to equilibrate shows that the liquid-solid phase transition in the system pulls to higher temperatures. Moreover, the MD simulation results show that the cooling rate chosen has a large effect on the microstructure of the system.

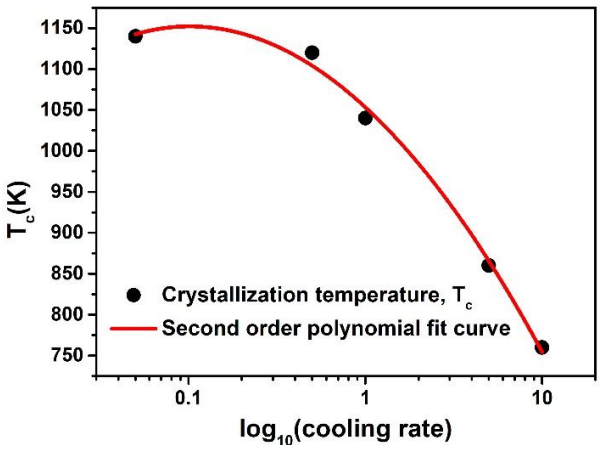

Fig. 2. *Change of T_c as a function of the logarithm of the cooling rate.*

In order to analyze the crystal-liquid and liquid-crystal phase transitions occurring in the system during the heating and cooling processes, we used *g(r)* curves, which are widely preferred in MD simulation methods. The form of *g(r)* used in MD simulations is as follows.

$$g(\mathrm{r}) = \frac{V}{N^2}\left\langle \sum_{i=1}^{n} \frac{n(\mathrm{r})}{4\pi r^2 \Delta r} \right\rangle \qquad (3)$$

Here *N*, *V* and *n(r)* show the number of atoms in the MD simulation box, the volume of the box, and the number of particles in the range *r* to *r* + *Δr*, respectively. In order to see the effect of the cooling rate on the temperature-dependent change of Rh's structure, the *g(r)* curves calculated for the slowest (0.05 K/ps) and fastest (10 K/ps) cooling rates at different temperatures are comparatively given in Figs. 3a-3b with the *g(r)* curves obtained during the heating process at the same temperatures. The results of other cooling rates are not shown here to avoid duplication. The heating curves given for 2700 K overlap with the *g(r)* curves obtained for both cooling rates. This indicates that the system is a liquid that has reached equilibrium at this temperature. Differences begin to occur in the peak heights and the positions of these peaks of the *g(r)* curves obtained from the heating and cooling process depending on the decreasing temperature. In the g(r) curves obtained for both cooling rates at lower temperatures, more pronounced and sharp peaks have been formed as in the ideal *FCC* structure during the heating process. The peaks of the curves obtained for 10 K/ps are shallower than those of the heating curves, while the *g(r)* at 900 and 300 K for 0.05 K/ps are in good agreement with the heating curves. These results show that crystal nucleation can develop more rapidly if the system is given enough time to equilibrate. Fig. 3(c) depicts the comparison of the calculated *g(r)* curves at 300 K for heating and five different cooling rates. From this figure, it can be clearly seen that all peak heights of the *g(r)* decrease with increasing cooling rate. These findings show that the cooling rate used has great effects on the crystal nucleation that occurs in the system and the development of this nucleation with decreasing temperature.

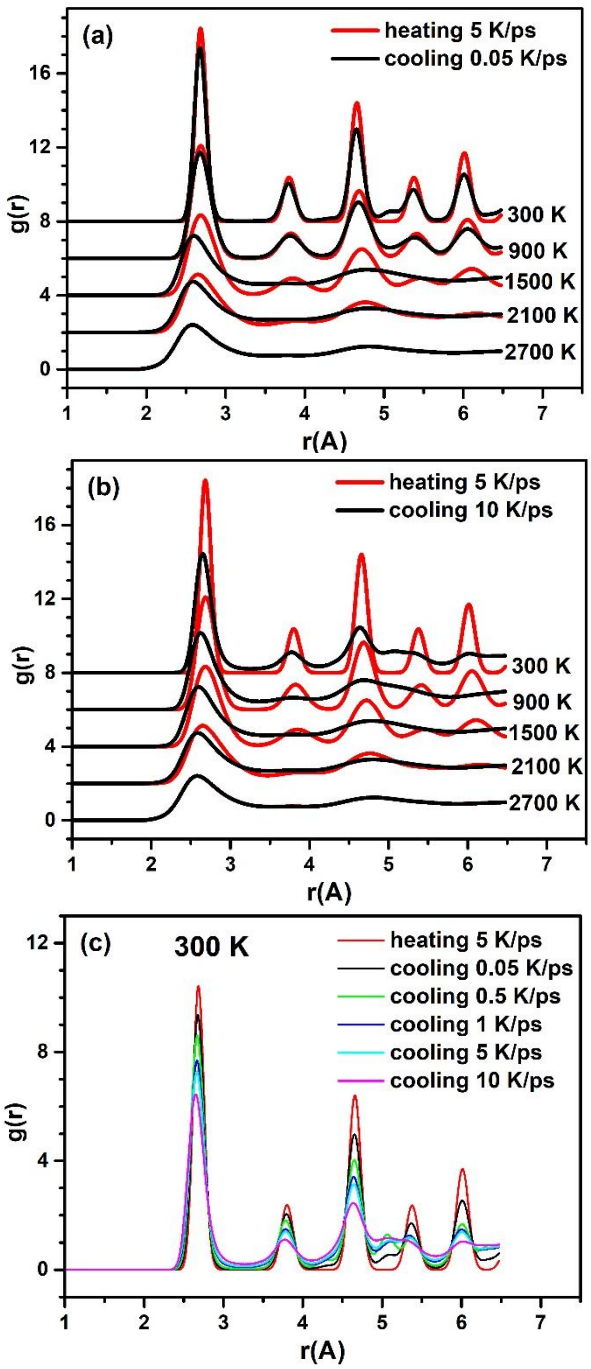

Fig. 3. *Comparison of the g(r) curves obtained at different temperatures with the cooling rates of (a) 0.05 K/ps and (b) 0.5 K/ps with the g(r) curves obtained from the heating process. (c) Heating and cooling g(r) curves at 300 K.*

We used the pair analysis (PA) method [11, 12] to better define the cooling rate-dependent liquid-solid phase transition. Readers can find more detailed information about this method in [1, 12–14] resources. We used OVITO software [15] for the visualization of the MD box and for PA. Snapshots of the simulation box at 300 K and the distribution of crystalline (or other) clusters for all cooling rates are given in Fig. 4. It has been observed that the fraction of FCC and HCP type clusters in the system increased as the cooling rate decreased. It is interesting that FCC type clusters are dominant for 0.05 K/ps while HCP type clusters are more dominant for 0.5 K/ps. These results are also an indication of what kind of effects the chosen cooling rate can have on the system.

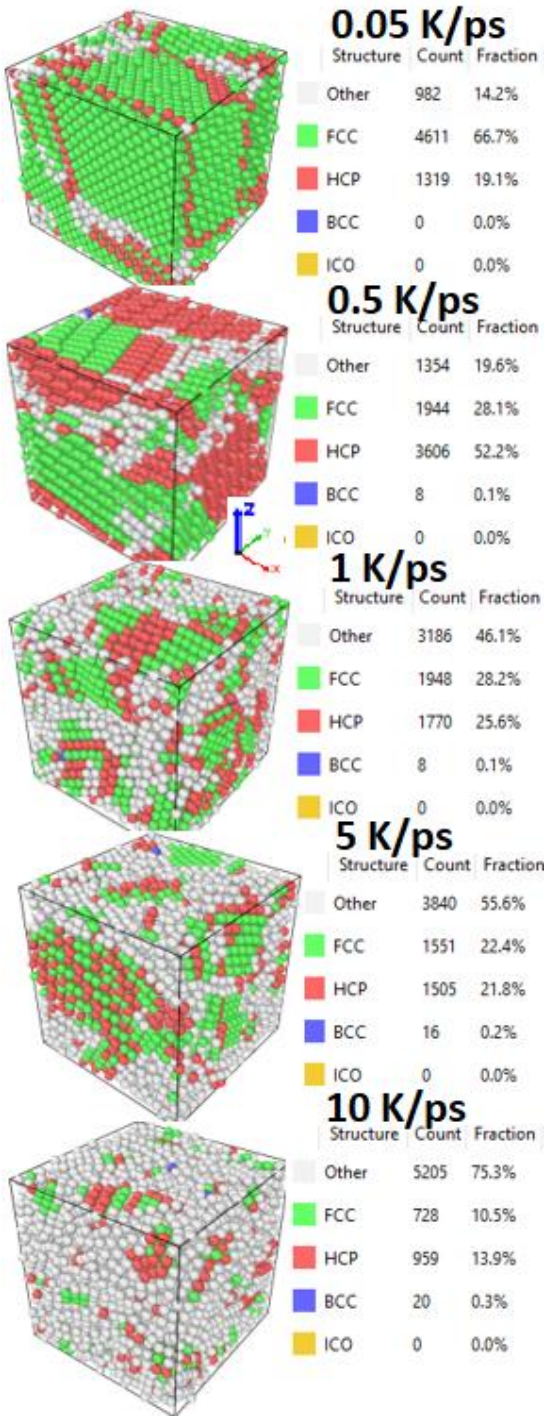

Fig. 4. *PA analysis results and snapshots at 300 K for five cooling rates.*

Figs. 5(a)-(b) show the variation of the PA fractions obtained for the fastest and slowest cooling rates as a function of temperature. It

can be clearly seen from the figures that the clusters we call "Other", which are mostly found in liquid systems at high temperatures, are dominant in both cooling rates. In both simulations, there has been a sudden increase in FCC and HCP type clusters during the liquid-solid phase transition and a sudden decrease in the number of "Other" clusters as a result. This means that during the cooling, the liquid Rh changes its phase, transforming into a FCC + HCP-like crystal structure. These results are also consistent with the results obtained and discussed for the g(r)s above. Fig. 5(c) presents a comparison of the PA results calculated at 300 K for five cooling rates. The slower the system is cooled, the higher the number of FCC and HCP crystal clusters. The predominance of FCC crystal clusters for 0.05 K/ps cooling rate may mean that if the system is cooled even more slowly, it may return to its ideal FCC structure. As a result, it has been observed that the cooling rate is very effective in the development of the atomic structure of the system, determination of the T_c and the formation of crystal clusters.

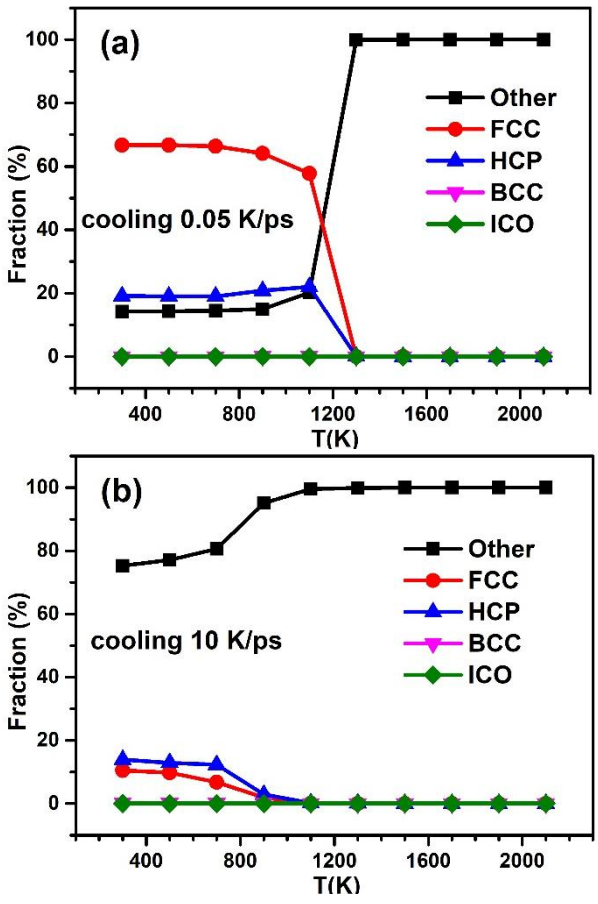

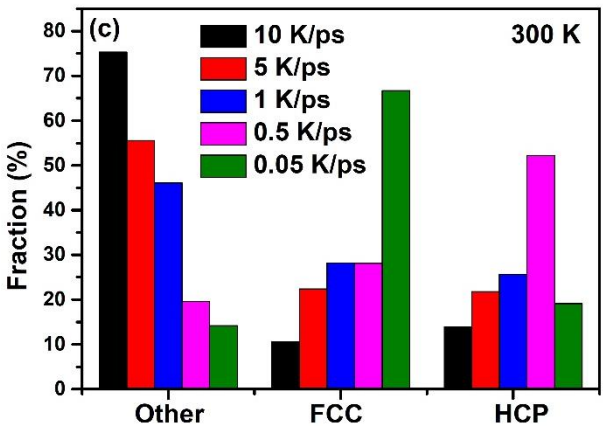

Fig. 5. *PA fractions as a function of temperature for (a) 0.05 K/ps and (b) 10 K/ps. (c) PA fractions at 300 K for five cooling rates.*

CONCLUSION

In the present study, changes in the atomic structure of Rh during the heating and cooling processes have been investigated by the MD simulations method using the EAM potentials. The liquid-crystal phase transition that occurred in the system during the cooling has been investigated using five different cooling rates. It has been observed that as the cooling rate decreased, the peak heights and positions of the *g(r)* curves of heating and cooling obtained at low temperatures were more consistent. Similarly, PA results show that FCC type crystal clusters are dominant in the slower cooled system. All these results show that the cooling rate in MD simulations has a significant influence on the structural development of the liquid Rh, the crystallization process and the evolution of its microstructure.

REFERENCE

[1] Çeltek M, Güder V. Sıvı Vanadyumun Kristalizasyon Sürecine Soğutma Oranı Etkisinin Moleküler Dinamik Benzetim Metodu ile İncelenmesi. Erzincan Üniversitesi Fen Bilim Enstitüsü Derg 2020; 13: 730–745.

[2] Celik FA. Molecular dynamics simulation of crystallization of amorphous aluminium modelled with EAM. Bitlis Eren Univ J Sci Technol 2012; 2: 44–48.

[3] Celtek M, Sengul S. The characterisation of atomic structure and glass-forming ability of the Zr–Cu–Co metallic glasses studied by molecular dynamics simulations. Philos Mag 2018; 98: 783–802.

[4] Celtek M, Sengul S. Thermodynamic and dynamical properties and structural evolution of binary Zr80Pt20 metallic liquids and glasses: Molecular dynamics simulations. J Non Cryst Solids 2018; 498: 32–41.
[5] Alder BJ, Wainwright TE. Phase Transition for a Hard Sphere System. J Chem Phys 1957; 27: 1208–1209.
[6] Mandell MJ, McTague JP, Rahman A. Crystal nucleation in a three- dimensional Lennard- Jones system. II. Nucleation kinetics for 256 and 500 particles. J Chem Phys 1977; 66: 3070–3075.
[7] Daw MS, Baskes MI. Embedded atom method: derivation and application to impurities,surfaces and other defects in metal. Phsical Rev B 1984; 29: 6443–6453.
[8] Sheng H. https://sites.google.com/site/eampotentials/Rh , Retrieved September 25, 2020.
[9] Smith W, Forester TR. DL_POLY_2.0: A general-purpose parallel molecular dynamics simulation package. J Mol Graph 1996; 14: 136–141.
[10] Kittel C. *Introduction to Solid State Physics*. New York: John Wiley & Sons Inc., 1986.
[11] Honeycutt JD, Andersen HC. Molecular Dynamics Study of Melting and Freezing of Small Lennard- Jones Clusters. J Phys Chem 1987; 91: 4950–4963.
[12] Çeltek M, Şengül S. Effects of cooling rate on the atomic structure and glass formation process of Co90Zr10 metallic glass investigated by molecular dynamics simulations. Turkish J Phys 2019; 43: 11 – 25.
[13] Sengul S, Celtek M. Pressure Effects on the Structural Evolution of Monatomic Metallic Liquid Hafnium. BEU J Sci 2018; 7: 144–158.
[14] Çeltek M, Şengül S, Dömekeli Ü. Hızlı Soğutma Sürecinde Dörtlü Zr48Cu36Ag8Al8 İri Hacimli Metalik Camının Atomik Yapısının Gelişimi. Süleyman Demirel Üniversitesi Fen Bilim Enstitüsü Derg 2019; 23: 954–962.
[15] Stukowski A. Visualization and analysis of atomistic simulation data with OVITO-the Open Visualization Tool. Model Simul Mater Sci Eng 2010; 18: 015012.